Interaction of Lipoprotein Lipase with *p*-Nitrophenyl *N*-Alkylcarbamates: Kinetics, Mechanism, and Analogy to the Acylenzyme Mechanism†

Hyeon-Cheol Shin and Daniel M. Quinn*

Department of Chemistry, The University of Iowa, Iowa City, Iowa 52242

Received May 8, 1991; Revised Manuscript Received October 14, 1991

ABSTRACT: The interaction of lipoprotein lipase with *p*-nitrophenyl *N*-alkylcarbamates [PNPOC(=O)-NHC_nH_{2n+1}; n = 4, 8, and 12] proceeds by the three-stage mechanism shown below. After reversible

$$E + C \underset{K_c}{\rightleftharpoons} EC \xrightarrow{k_c} EC' + P \xrightarrow[H_2O]{k_d} E + Q$$

formation of the enzyme–carbamate complex (EC), rapid carbamylation (k_c) precedes slow decarbamylation. Therefore, in short-term assays (≤30 min) of lipoprotein lipase catalyzed hydrolysis of *p*-nitrophenyl butyrate, activity is rapidly lost. The inhibition by *p*-nitrophenyl *N*-butylcarbamate follows saturation kinetics, which allows determination of $K_c = 5.4 \pm 0.9$ μM and $k_c = (4.9 \pm 0.7) \times 10^{-2}$ s^{-1}. Saturation kinetics are not observed for the longer inhibitors *p*-nitrophenyl *N*-octylcarbamate and *p*-nitrophenyl *N*-dodecylcarbamate. Rather, plots of the pseudo-first-order rate constant for activity loss versus inhibitor concentration are concave upward, consistent with inhibitor binding to two sites on the enzyme. The inhibition phase is sufficiently rapid that *p*-nitrophenyl *N*-octylcarbamate can be used to titrate enzyme active sites. On the other hand, long-term assays (>5 h) show sequential inhibition and activity return phases, and from the activity return phase k_d is calculated. The long-term activity time course is accurately simulated by Runge–Kutta integration of the differential equations for the three-stage mechanism. These approaches have been used to characterize the kinetics of interaction of the enzyme with the carbamate inhibitors. Because the three-stage mechanism is equivalent in form to the acylenzyme mechanism for lipoprotein lipase action, the results described herein provide information on the fatty acyl specificity of the enzyme in the acylation and deacylation stages of catalysis.

Lipoprotein lipase (LpL,[1] EC 3.1.1.34) is a lipolytic enzyme that is bound to the capillary endothelium, where it catalyzes the catabolic conversion of triacylglycerol-rich lipoproteins to smaller, cholesteryl ester-rich remnant lipoproteins [for reviews, see Borensztajn (1987), Olivecrona and Bengtsson (1984), Quinn et al. (1983), and Smith and Pownall (1984)]. Because LDL is a product of LpL catabolism, as are highly atherogenic chylomicron and VLDL remnants (Zilversmit, 1977, 1979), the enzyme plays a crucial role in cardiovascular metabolism and health. Despite this, the chemical mechanism of LpL action was until recently more conjecture than enzymology. In the early 1980s an acylenzyme mechanism for LpL catalysis was suggested (Quinn et al., 1983; Vainio et al., 1982) that is reminiscent of the mechanism of serine protease catalysis (Stroud, 1974; Blow, 1976; Kraut, 1977; Polgar, 1987). However, this suggestion was based only on the observations that compounds that are irreversible inhibitors (e.g., PMSF) and reversible transition-state analogue inhibitors (e.g., boronic acids) of serine proteases are also LpL inhibitors.

Several developments since 1986 now put the LpL acylenzyme mechanism, as outlined in Scheme I, on a firm footing. Burdette and Quinn (1986) trapped the lauroyl-LpL intermediate that forms during turnover of mixed micellar *p*-nitrophenyl laurate with NH_2OH. This nucleophile provides a deacylation route that is alternate to the hydrolytic step of Scheme I, which thereby increases V_{max}. The amino acid sequences of several LpLs have been deduced from the requisite cDNA sequences (Enerbäck et al., 1987; Kirchgessner et al., 1987; Wion et al., 1987), which include that of bovine milk LpL (Senda et al., 1987), the enzyme used in the studies described herein. The LpL sequences place the enzyme in a gene family that contains, among other important lipolytic enzymes, pancreatic lipase and hepatic lipase (Komaromy & Schotz, 1987). The enzymes in this family have conserved serine, histidine, and aspartate residues that are putative components of active site charge-relay systems like those of the serine proteases. This suggestion is supported by a third important observation. Two recent papers describe the crystal structures of *Mucor miehie* lipase (Brady et al., 1990) and

Chart I: Carbamate Inhibitors of LpL[a]

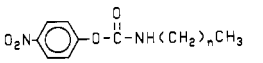

[a] n = 3, *p*-nitrophenyl *N*-butylcarbamate (PNPBC); n = 7, *p*-nitrophenyl *N*-octylcarbamate (PNPOC); n = 11, *p*-nitrophenyl *N*-dodecylcarbamate (PNPDC).

† This work was supported by NIH Grant HL30089. D.M.Q. was the recipient of a Research Career Development Award (HL01583, 1985–90).

* To whom correspondence should be addressed.

[1] Abbreviations: ANS, 8-anilino-1-naphthalenesulfonic acid; CI-MS, chemical ionization mass spectroscopy; CMC, critical micelle concentration; GC–MS, gas chromatography–mass spectroscopy; LDL, low density lipoprotein; LpL, lipoprotein lipase; NMR, nuclear magnetic resonance; PMSF, phenylmethanesulfonyl fluoride; PNPB, *p*-nitrophenyl butyrate; PNPBC, *p*-nitrophenyl N-butylcarbamate; PNPDC, *p*-nitrophenyl *N*-dodecylcarbamate; PNPOC, *p*-nitrophenyl *N*-octylcarbamate; TLC, thin-layer chromatography; TMS, tetramethylsilane; TX100, Triton X100; VLDL, very low density lipoprotein. The single-letter amino acid codes used are C, cysteine; D, aspartate; H, histidine; and S, serine.

0006-2960/92/0431-811$03.00/0

Scheme I: Mechanism of LpL Catalysis

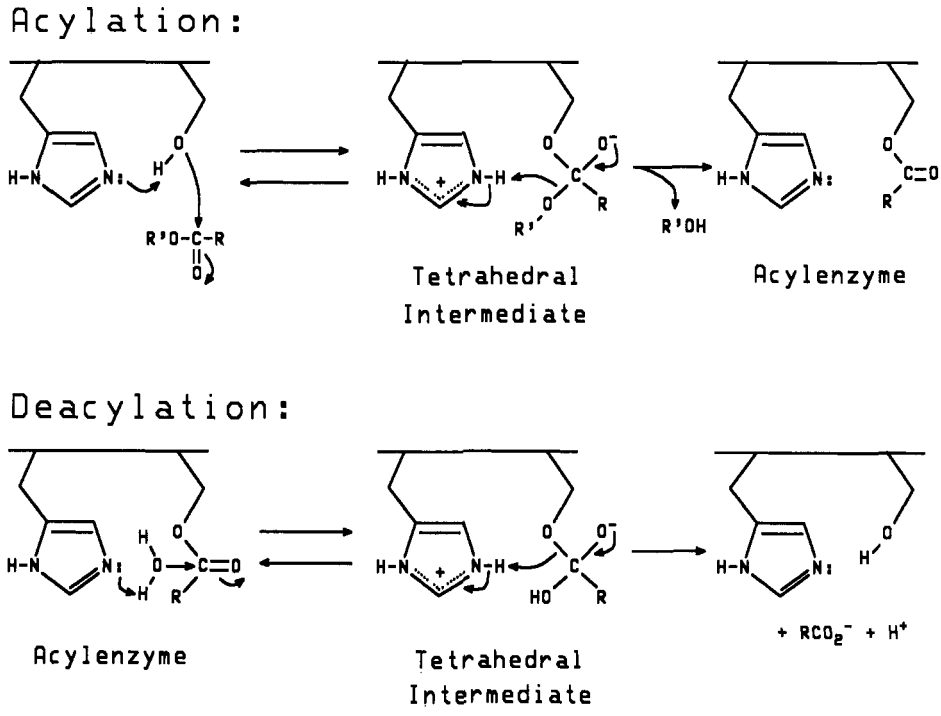

human pancreatic lipase (Winkler et al., 1990). Both enzymes have active site D-H-S triads that closely align stereochemically with the active sites of serine proteases. The residues that contribute to the triad in pancreatic lipase are S152, H263, and D176. The pancreatic lipase structure effectively ends the controversy over whether S152 is the active site serine and creates serious doubt that G-X-S-X-G is the "interfacial binding site" of lipases (Verger, 1984; Chapus & Sémériva, 1976; Guidoni et al., 1981). More important for the studies described in this paper, the pancreatic lipase active site triad is conserved in the various LpL sequences; the corresponding residues in bovine LpL are S134, H243, and D158 (Senda et al., 1987).

Now that the broad strokes of the LpL mechanism have been clarified, one can ask questions about the nature and control of the enzyme's activity. For example, in which of the stages of the reaction, acylation or deacylation, is substrate specificity, in particular, fatty acyl specificity, expressed? In this paper we described the interaction of LpL with the carbamates in Chart I. Inhibition of bovine milk LpL by *p*-nitrophenyl *N*-butylcarbamate (i.e., $n = 4$) was originally described by Twu et al. (1976). The carbamates of Chart I provide a reaction system with which the question raised above, and many others, can be addressed.

Materials and Methods

Materials. LpL was isolated from skimmed bovine milk by affinity chromatography on heparin–Sepharose (Iverius, 1971), as described by Matsuoka et al. (1980). Protein concentrations were determined by the Bradford method (1976). *p*-Nitrophenyl butyrate (PNPB), *p*-nitrophenyl chloroformate, TX100, 8-anilino-1-naphthalenesulfonic acid (ANS), taurocholic acid, and heparin from porcine intestinal mucosa were purchased from Sigma Chemical Co., and D_2O and dodecylamine were purchased from Aldrich Chemical Co. and Fluka Chemie AG, respectively. ANS was recrystallized from ethanol before use. Water for buffer preparation was distilled and deionized by passage through a mixed-bed ion-exchange column (Barnsted, Sybron Corp.). All other materials were commercial reagent grade products.

Synthesis of Carbamate Inhibitors. The *N*-butyl and *N*-octyl carbamates PNPBC and PNPOC were synthesized as described by Hosie et al. (1987). The synthesis of *p*-nitrophenyl *N*-dodecylcarbamate (PNPDC) was achieved by a modification of these procedures. Dodecylamine (0.02 mol) in 15 mL of CH_2Cl_2 was added over a period of 40 min to a 15-mL solution of *p*-nitrophenyl chloroformate (0.01 mol) in the same solvent, and the mixture was stirred overnight at room temperature. The CH_2Cl_2 solution was washed with 65 mL of water, 65 mL of 0.1 N HCl, and then 65 mL of water and then dried over $MgSO_4$; this washing procedure was repeated. The CH_2Cl_2 solution was rotoevaporated to dryness, and the resulting solid was recrystallized from methanol to afford white, sheet-like crystals: mp 92–94 °C. The product gave a single spot on TLC in 8:2 hexane/ethyl acetate (v/v), $R_f = 0.33$. CI-MS, run on a Nermag R10-10C GC–MS, showed an M + 1 peak at m/e 351, in agreement with the calculated molecular weight of 350. The ^1H NMR spectrum, acquired in $CDCl_3$ on a JEOL FX90Q spectrometer operating at 90 MHz, showed the following features, in parts per million relative to TMS as internal standard: 0.88, CH_3; 1.26, $(CH_2)_9$; 1.54, $NHCCH_2$-; 3.29, $NHCH_2$-; 7.26, 7.36, 8.18, and 8.28, doublet of doublets from phenyl protons.

Inhibition Kinetics. LpL-catalyzed hydrolysis of PNPB was monitored at 400 nm on Beckman DU40 or HP8452A UV–visible spectrophotometers that are interfaced to IBM PC computers. Reaction temperature was controlled to ±0.1 °C by using circulating, refrigerated water baths to circulate water through the cell holders of the spectrophotometers. Reactions in H_2O were performed in 0.1 M sodium phosphate buffer, pH 6.94, that contained 0.1 N NaCl. Reactions in D_2O were performed in an equivalent buffer (Schowen, 1978) of pD 7.47. Buffer pH and pD values were measured on a Corning 125 pH meter that is equipped with a glass combination electrode; the pD of D_2O buffers was calculated by adding 0.4 to the pH meter reading (Schowen, 1978; Salomaa et al., 1964). Additional components of assay mixtures are specified in figure legends and table footnotes throughout this paper.

Carbamates rapidly inhibit LpL (≤30 min), and the time course for loss of LpL activity was characterized by using the

PNPB assay described in the preceding paragraph. Both continuous and stopped-time inhibition assays were performed. In the continuous assay, which was described by Hosie et al. (1987), the time course for PNPB turnover was determined in the absence (control) and presence of the inhibitor. The first derivatives of the control and inhibition time courses were calculated by the method of Savitsky and Golay (1964); these derivatives are measures of the instantaneous LpL activity. The percent activity remaining is calculated by dividing the activity at various times of the inhibition time course by activities of the control time course at the same absorbance. PNPB hydrolyzes slowly in the absence of LpL, with a first-order rate constant of $k_b = 9.5 \times 10^{-6}$ s^{-1}. The activities determined at different times of the control and inhibition time courses were corrected by subtracting k_b[PNPB], the component due to background hydrolysis of the substrate. The pseudo-first-order inhibition rate constant is calculated by fitting the resulting data to eq 1 by nonlinear least-squares

$$\%A = (\%A_0 - \%A_{inf})e^{-kt} + \%A_{inf} \quad (1)$$

procedures (Wentworth, 1965). In this equation $\%A$, $\%A_0$, and $\%A_{inf}$ are percent activities at times t, 0, and infinity, and $k = k_c^{obsd}$ is the observed rate constant. In the stopped-time assay, LpL is incubated with an inhibitor and, at various times, aliquots are withdrawn and residual activity is determined by measuring initial rates of PNPB hydrolysis. Initial rates are calculated by linear least-squares fitting of time courses that comprise <10% of total substrate turnover. The activities are divided by those measured in the absence of inhibitor (control), and the resulting data are fit to eq 1. The stopped-time assay was also used to measure the first-order rate constant for spontaneous LpL inactivation in the absence of inhibitor.

Because of the rapidity of inhibition by PNPOC, inhibitor concentrations comparable to that of LpL were sometimes used, and thus the inhibition kinetics were second order. In this situation, the second-order inhibition rate constant $k = k_c/K_c$ was calculated by fitting data to eq 2 by nonlinear

$$\%A = \frac{100([C]_0 - [E]_0)}{[C]_0 e^{kt([C]_0-[E]_0)} - [E]_0} \quad (2)$$

least-squares procedures (Wentworth, 1965). In this equation, $[C]_0$ and $[E]_0$ are the initial concentrations of carbamate inhibitor and LpL, respectively.

Active Site Titration. Because of the rapidity of inhibition by PNPOC, the carbamate can be used to titrate the active sites of LpL. Percent activity remaining was measured at the completion of the rapid inhibition phase on incubation of the enzyme with a range of concentrations of PNPOC. A plot of residual activity versus [PNPOC] is linear when the concentration of the carbamate is less than that of LpL active sites, and extrapolation of the plot to its x-axis intercept gives the molar concentration of active sites.

Micelle Assays. Three methods were employed to detect the formation at 25 °C of micelles of the *N*-alkylcarbamate inhibitors in the same buffer as used for inhibition experiments. The first method involved measuring the rise in a capillary of 0.3-mm inside diameter of solutions of the carbamate. The height of the rise depends on the surface tension of the analyte solution, which changes abruptly as the CMC is passed. In our hands the capillary rise method detects the aggregation of amphipathic molecules that form micelles of high aggregation number, such as TX100. The measured CMC = 0.38 ± 0.01 mM compares reasonably well with the CMC = 0.20 ± 0.05 mM reported by Burdette and Quinn (1986). The capillary rise method also detects the aggregation of sodium taurocholate, a bile salt that forms micelles of low aggregation number [measured CMC = 4 ± 1 mM; literature CMC = 3.3 mM and 3.1 mM, respectively, at 20 °C and 30 °C and at comparable ionic strength (Carey & Small, 1969)]. No micelle formation was detected by this method for 0–10 μM solutions of PNPOC or PNPDC. The second method involved measuring the enhancement of fluorescence emission of 100 nM ANS in the presence of micelles of the amphipathic analyte (Andley & Chakrabarti, 1981). In our hands this method gives a CMC = 0.20 ± 0.03 mM for TX100, again in good agreement with the literature value. Micelle formation in solutions of 0–10 μM PNPOC was not detected by this method. The third method involved measuring the fluorescence at 311 nm of carbamate solutions on excitation at 283 nm, with the expectation that the emission maximum wavelength and/or the emission intensity would change as micelles formed. This method failed to detect micelles in 0–1 μM solutions of PNPOC. All fluorescence measurements were performed on an SLM Aminco SPF-500C spectrofluorometer. In summary, one must conclude that carbamate micelles do not form in the concentration ranges employed for the inhibition experiments.

Runge–Kutta Integration. In long-term assays (≥5 h) rapid inhibition is followed by slow recovery of activity, due apparently to hydrolytic turnover of the carbamyl-LpL intermediate. In control experiments, carbamate inhibitors were found to spontaneously hydrolyze and LpL was found to spontaneously lose activity in first-order reactions. These processes are outlined in reaction eqs 3–5, which are described by differential eqs 6–8. Equation 3 represents sequential

$$E + C \xrightarrow{k_c/K_c} EC' + P \xrightarrow[H_2O]{k_d} E + Q \quad (3)$$

$$E \xrightarrow{k_i} E_i \qquad EC' \xrightarrow{k_i} E_i \quad (4)$$

$$C \xrightarrow[H_2O]{k_h} P + Q \quad (5)$$

$$d[E]/dt = k_d[EC'] - (k_c/K_c[C] + k_i)[E] \quad (6)$$

$$d[C]/dt = -(k_h + k_c/K_c[E])[C] \quad (7)$$

$$d[EC']/dt = k_c/K_c[E][C] - (k_d + k_i)[EC'] \quad (8)$$

carbamylation and decarbamylation of LpL. In eq 4, it is assumed that both free LpL and the carbamylated intermediate spontaneously lose activity with the same rate constant k_i. Spontaneous carbamate hydrolysis is represented by eq 5.

Differential eq 6 was integrated numerically to determine the time function of [E]. Calculations were performed on an IBM compatible microcomputer that has an 80386 processor and 80387 math coprocessor; the requisite program was written, compiled, and executed by using the TURBO BASIC software package (Borland International, Scotts Valley, CA). Because [E], [EC'], and [C] are all involved in eq 6, differential eqs 6–8 were integrated simultaneously by using fourth-order Runge–Kutta integration (Carpenter, 1984). According to this method, the species concentrations at time j along the LpL activity time course are given by

$$[E]_j = [E]_{j-1} + (e_{1j} + 2e_{2j} + 2e_{3j} + e_{4j})/6 \quad (9)$$

$$[C]_j = [C]_{j-1} + (c_{1j} + 2c_{2j} + 2c_{3j} + c_{4j})/6 \quad (10)$$

$$[EC']_j = [EC']_{j-1} + (ec'_{1j} + 2ec'_{2j} + 2ec'_{3j} + ec'_{4j})/6 \quad (11)$$

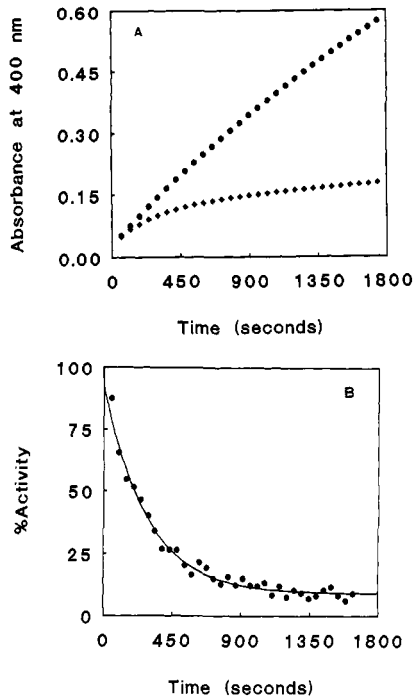

FIGURE 1: Continuous assay of inhibition of LpL by *p*-nitrophenyl *N*-butylcarbamate (PNPBC). (A) Time courses are shown for LpL-catalyzed hydrolysis of PNPB in the presence (◆) and absence (●) of 0.4 μM PNPBC. Reactions were run at 25.0 ± 0.1 °C in 1.00 mL of 0.1 M sodium phosphate buffer, pH 6.94, that contained 0.1 N NaCl, 100 μg of heparin, 2.4 μg of LpL, 2% (v/v) CH_3CN, 0.5% (v/v) glycerol, and $[PNPB]_0$ = 0.4 mM. (B) The first-order decrease in the percent activity of LpL effected by 0.4 μM PNPBC is depicted. Percent activities were calculated from the time courses displayed in panel A, as described in the Materials and Methods section. The curved line is a fit to eq 1 of the text.

The concentration increments, e_{ij}, in eq 9 are defined in the equations

$$e_{1j} = \{k_d[EC']_{j-1} - (k_c/K_c[C]_{j-1} + k_i)[E]_{j-1}\}\theta_t \quad (12)$$

$$e_{2j} = \{k_d([EC']_{j-1} + ec'_{1j}/2) - (k_c/K_c([C]_{j-1} + c_{1j}/2) + k_i)([E]_{j-1} + e_{1j}/2)\}\theta_t \quad (13)$$

$$e_{3j} = \{k_d([EC']_{j-1} + ec'_{2j}/2) - (k_c/K_c([C]_{j-1} + c_{2j}/2) + k_i)([E]_{j-1} + e_{2j}/2)\}\theta_t \quad (14)$$

$$e_{4j} = \{k_d([EC']_{j-1} + ec'_{3j}) - (k_c/K_c([C]_{j-1} + c_{3j}) + k_i)([E]_{j-1} + e_{3j})\}\theta_t \quad (15)$$

Equation 12 is a finite difference analogue of differential eq 6, in which the finite time step is defined as θ_t; eqs 13–15 are similar in form, save that the concentrations are increased by using concentration increments calculated in the respective preceding equations. Similar sets of equations are written for c_{ij} and ec'_{ij} by referring to differential eqs 7 and 8. For integration of continuous inhibition assays, θ_t = 30 s was used. The values of θ_t for stopped-time assays were 60, 30, and 90 seconds, respectively, for inhibitions by PNPBC, PNPOC, and PNPDC.

In eq 9 the concentration of active LpL at time j is the sum of the active LpL concentration at time $j - 1$ (one time step θ_t earlier) and a weighted average of concentration increments e_{ij}. Concentrations of C and EC′ are computed in a similar fashion in eqs 10 and 11. The concentrations of E, C, and EC′ are set at $[E]_0$, $[C]_0$, and 0, respectively, at time = 0, and the first set of concentrations calculated according to eqs 9–11 is that which is one time step θ_t after the beginning of the reaction. The computation is continued until the end of the inhibition time course is reached. The calculation is carried out by using an initial set of guesses of the rate constants k_c/K_c, k_d, k_i, and k_h and is continued over a grid of sets of these rate constants. For each rate constant set of the grid, the summed-squared-variance (SSV) was calculated from

$$SSV = \sum_j^n (\%A_{calcd} - \%A_{obsd})^2 \quad (16)$$

$\%A_{calcd}$ and $\%A_{obsd}$ are the respective calculated and observed percent activities, and the summation is carried out over all n values of the observed percent activity. The relation between percent activities and LpL concentration is given by eq 17, in

$$\%A = 100[E]/[E]_0 \quad (17)$$

which [E] is the active LpL concentration at time $j\theta_t$ and $[E]_0$ is the initial LpL concentration. That which minimizes SSV is taken as the set of best estimates of the rate constants.

Scheme II: Mechanism for Carbamylation of LpL

$$E + C \underset{k_2}{\overset{k_1}{\rightleftharpoons}} EC \xrightarrow{k_c} EC' + P \xrightarrow[H_2O]{k_d} E + Q$$

Table I: Rate Constants for Interaction of Lipoprotein Lipase and *p*-Nitrophenyl *N*-Alkylcarbamates

carbamate	k_c/K_c (M^{-1} s^{-1})	$10^5 k_d$ (s^{-1})	$10^4 k_h$ (s^{-1})
PNPBC	9000 ± 700[a]	2.1 ± 0.2[a]	3.4 ± 0.4[a]
	13300[b]	2.5[b]	3.7[b]
	9000 ± 2000[c]		
PNPOC	30000 ± 10000[a]	2.0 ± 0.4[a]	1.6 ± 0.6[a]
	15000[b]	4.3[b]	0.9[b]
	13000 ± 1000[d]		
PNPDC	1680 ± 70[d]	1.9 ± 0.4[a]	0.4 ± 0.1[a]
	4000[b]	2.8[b]	0.14[b]

[a] Calculated by Runge–Kutta integration of continuous long-term time courses. Values are means ± standard errors of four observations for PNPBC and of three observations for PNPOC. For PNPDC, values are means ± half the range of duplicate observations. [b] Calculated by Runge–Kutta integration of time courses determined by stopped-time assay. The time-course lengths were 24 h for PNPBC (cf. Figure 4B), 28 h for PNPOC, and 40 h for PNPDC. [c] Calculated by fitting the dependence of k_c^{obsd} on [PNPBC] to eq 18. The fit parameters were k_c = 0.049 ± 0.007 s^{-1} and K_c = 5.4 ± 0.9 μM. [d] Calculated from the linear portion of the dependence of k_c^{obs} on carbamate concentration; cf. Figure 2 for PNPOC.

Results

Figure 1A shows an overlay of time courses for LpL-catalyzed hydrolysis of PNPB in the absence (control) and the presence of 0.4 μM PNPBC. The damping of the slope of the reaction in the presence of PNPBC, versus the control, provides a clear indication of rapid inhibition of LpL activity. When the time dependence of the loss in LpL activity in the presence of the carbamate is computed as described in the Materials and Methods section, the plot in Figure 1B results. Nonlinear least-squares fitting (Wentworth, 1965) of these data to eq 1 shows that activity loss is well-described by first-order kinetics, with k_c^{obsd} = (3.35 ± 0.05) × 10^{-3} s^{-1}. Furthermore, the dependence of k_c^{obsd} on [C] is nonlinear and well described by saturation kinetics. That is, the inhibition phase of interaction of LpL with PNPBC proceeds by the mechanism given in Scheme II. In this scheme P is *p*-nitrophenoxide, Q is an *N*-alkylcarbamic acid, and EC is the noncovalent LpL-carbamate complex that precedes the chemical step(s) that produce the carbamylenzyme EC′. From this mechanism, the following equation emerges when $k_c \gg k_d$:

$$k_c^{obsd} = \frac{k_c[C]}{K_c + [C]} \quad (18)$$

In this equation, $K_c = k_2/k_1$. This equation is the inhibition

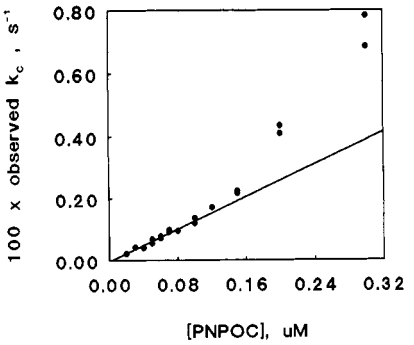

FIGURE 2: Dependence of first-order rate constant on carbamate concentration for inhibition of LpL by *p*-nitrophenyl *N*-octylcarbamate (PNPOC). Reaction conditions were as described in the legend of Figure 1, save that [PNPOC] was varied as shown and reactions contained 5.5 μg of LpL. The rate constants at [PNPOC] $\leq$ 0.1 μM were calculated by multiplying second-order inhibition rate constants by $[PNPOC]_0$. Second-order inhibition rate constants were calculated by fitting inhibition time courses to eq 2 in the Materials and Methods section.

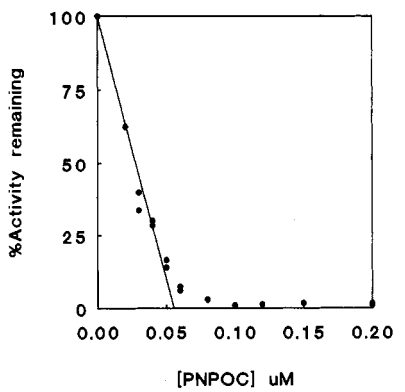

FIGURE 3: Titration of LpL active sites by inhibition with *p*-nitrophenyl *N*-octylcarbamate (PNPOC). Reactions conditions were as described in the legend of Figure 1, save that [PNPOC] was varied as shown and reactions contained 5.5 μg of LpL. The residual percent LpL activity after the rapid inhibition phase is plotted vs [PNPOC]. Linear extrapolation of the least-squares fit of the rapidly descending portion of the plot to the *x*-axis gives a concentration of viable LpL active sites of 56 $\pm$ 2 nM.

analogue of the Michaelis–Menten equation (Kitz et al., 1967). The data for the dependence of k_c^{obsd} on [C] were fit to eq 18, and the results are gathered, along with other results, in Table I.

The inhibition kinetics are somewhat different for the C_8 and C_{12} carbamates, PNPOC and PNPDC, respectively. Inhibitions are again rapid, but the dependence of k_c^{obsd} on [C] is linear at the lower inhibitor concentrations, as shown in Figure 2 for interaction of LpL with PNPOC. At the higher concentrations the dependence of k_c^{obsd} on [C] breaks upward, and thus the inhibition rate is enhanced. The failure of three different assays to detect micelles of PNPOC (cf. Materials and Methods) indicates that this unusual behavior is not due to aggregation of the carbamate. This upward-breaking dependence of inhibition rate constant on [C] is yet more dramatic for interaction of LpL with PNPDC (data not shown). Therefore, at the lower carbamate concentrations no saturation of LpL as the EC complex occurs, eq 18 reduces to a linear dependence on [C], and only k_c/K_c is determined from the slope of the plot. These values for the C_8 and C_{12} carbamates are gathered in Table I. Inhibition by 0.2 μM PNPOC was also measured in D_2O buffer, from which a solvent isotope effect of 1.5 $\pm$ 0.1 on k_c^{obsd} was obtained.

A slow recovery of LpL activity follows rapid inhibition, and is accounted for in Scheme II by the hydrolytic decarbamylation step k_d. Therefore, *p*-nitrophenyl *N*-alkylcarbamates are not true irreversible inhibitors of LpL, but rather they are slow substrates whose sluggishness is accounted for by rate-determining decarbamylation.

Because of the rapidity of carbamylation, PNPOC was used to titrate the active sites of LpL, as shown in Figure 3. The LpL concentration calculated as the *x*-axis intercept of this figure is 63 $\pm$ 6% of the expected concentration on the basis of enzyme mass. This result is not particularly sensitive to the region of the rapidly descending portion of the plot that is chosen for least-squares analysis. When the analysis was over the range 0–40 nM, 0–50 nM, or 0–60 nM PNPOC, the value was 60%, 63%, or 66%, respectively, of the expected LpL concentration. This result shows not only that carbamylation produces a 1:1 complex with LpL but also that the enzyme preparation is reasonably clean. Since the titration required only 5.5 μg of LpL, active site titration with *p*-nitrophenyl *n*-alkylcarbamates constitutes a convenient analytical method for characterizing purified enzyme samples.

Factors in addition to those shown in Scheme II must be taken into account to describe the overall kinetics of interaction of LpL with *p*-nitrophenyl *N*-alkylcarbamates. During long-term assays of LpL carbamylation and decarbamylation the inhibitor is depleted and LpL spontaneously loses activity. The set of differential equations for d[E]/dt, d[EC′]/dt, and d[C]/dt that describe these various processes does not yield to analytical solution. Therefore, the differential equations were integrated by the Runge–Kutta method (Carpenter, 1984); the requisite mathematics are outlined in the Materials and Methods section. Figure 4A shows the Runge–Kutta integration of the time course for LpL activity, determined by the continuous assay method, on interaction with PNPBC. The time course shows distinct inhibition, steady-state (i.e., constant activity) and activity return phases. Because of substrate depletion, this assay could not be continued past 5 h. The stopped-time assay displayed in Figure 4B circumvents this limitation and again shows rapid inhibition followed by activity return. Also displayed is the plot of spontaneous loss of LpL activity, from which it is clear that the carbamylated enzyme regains essentially 100% activity. There is therefore no need to account for appreciable irreversible loss of LpL activity by, for example, nucleophilic expulsion of the amino group of the carbamyl-LpL intermediate by H243 of the active site. The rate constant for spontaneous loss of LpL activity was calculated by fitting the triangles of Figure 4B to a first-order kinetics equation; three such experiments gave a value of $k_i = (7 \pm 3) \times 10^{-6}$ s^{-1}, which corresponds to a half-life of 28 h. The values for the other rate constants determined by Runge–Kutta integration are insensitive to variation in k_i. For example, when k_i was constrained at various values in the range 1×10^{-6} to 3×10^{-5} s^{-1} for the integration shown in Figure 4A, k_c/K_c (=9200 M^{-1} s^{-1}) did not change, and k_d varied only in the range $(1.6–2.88) \times 10^{-5}$ s^{-1}, with an average value of $(2.1 \pm 0.4) \times 10^{-5}$ s^{-1}. The average k_d value from four separate experiments has the same value, as shown in Table I. Other rate constants determined from Runge–Kutta integrations of inhibition experiments with the various carbamates are also contained in the table.

Discussion

Broad substrate specificity is a hallmark of LpL catalysis (Quinn et al., 1983; Olivecrona & Bengtsson-Olivecrona, 1987; Smith & Pownall, 1984). The enzyme catalyzes the hydrolysis of numerous lipid substrates, such as triacylglycerols, 1,2- and 1,3-diacylglycerols, 1(3)-monoacylglycerols, phosphatidylcholines, and phosphatidylethanolamines. In addition, LpL

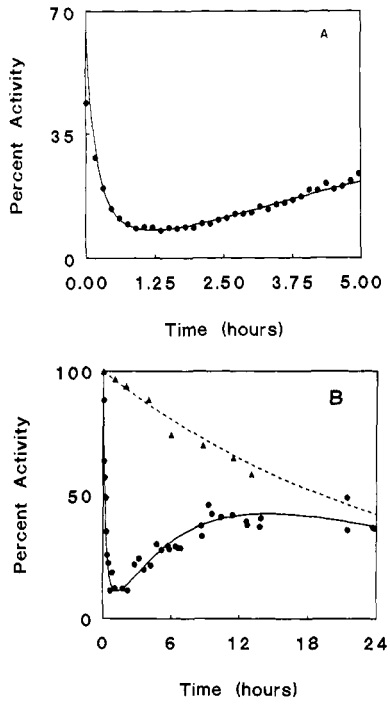

FIGURE 4: Long-term time courses for the interaction of LpL with *p*-nitrophenyl *N*-butylcarbamate (PNPBC) show sequential rapid inhibition, steady-state (constant activity), and activity return phases. Except where indicated, reaction conditions were as described in the legend of Figure 1. The nonlinear fits (solid lines) were generated by Runge–Kutta integration, as described in the Materials and Methods section. (A) LpL activities were determined by the continuous assay method (cf. Materials and Methods). Reactions contained 5.5 μg of LpL, $[PNPBC]_0 = 0.2$ μM, and $[PNPB]_0 = 0.2$ mM. (B) LpL activities were determined by the stopped-time assay method (cf. Materials and Methods). LpL (5.5 μg mL^{-1}) was incubated with 0.1 μM PNPBC, and at the indicated times 980-μL aliquots were removed and assayed by measuring initial velocities of hydrolysis of 0.2 mM PNPB. The dashed line is a least-squares fit of the spontaneous inactivation of LpL (▲) to the equation $\%A = 100e^{-k_i t}$, from which a rate constant $k_i = (1.0 \pm 0.1) \times 10^{-5}$ s^{-1} was determined. Two additional measurements at 26.5 and 27.1 h that were included in the least-squares analysis but are not shown on the plot gave LpL activities of 43% and 41%, respectively.

hydrolyzes nonphysiological substrates, such as *p*-nitrophenyl esters (Quinn et al., 1982; Burdette & Quinn, 1986; Egelrud & Olivecrona, 1973) and thioester analogues of acylglycerols (Shinomiya et al., 1984). A second hallmark of LpL action is the tremendous catalytic power of the enzyme. For example, LpL accelerates the hydrolysis of the nonphysiological substrate PNPB by a factor of 2×10^{11} (Sutton et al., 1986), which corresponds to a release of 15.4 kcal mol^{-1} of transition-state binding energy. Since the nonenzymic hydrolysis of lipid substrates occurs very slowly, if at all, the catalytic power that LpL brings to bear in physiological catalysis is likely much greater than for PNPB turnover. As our understanding of the microscopic molecular events in LpL action increases, a clearer picture of the origins of substrate specificity and catalytic power should emerge.

The carbamylenzyme mechanism that is characterized herein provides a unique level of resolution of microscopic events in LpL catalysis. In order to use the carbamylation and decarbamylation kinetics as probes of the factors that control the activity of LpL, one must be convinced that the carbamylenzyme and acylenzyme mechanisms are similar. There are several observations that suggest that this is the case: (a) the carbamylation rate constant k_c/K_c is highest for the carbamate of intermediate chain length (cf. Table I). A similar dependence of the acylation rate constant k^*_{cat}/K^*_m on chain length has been described by Burdette and Quinn (1986) for LpL-catalyzed hydrolysis of lipid *p*-nitrophenyl esters. (b) The rate of LpL-catalyzed hydrolysis of phosphatidylcholines decreases as the acyl chain is lengthened from C_{12} to C_{18} (Shinomiya et al., 1983), which mirrors the trends just cited for *p*-nitrophenyl esters and carbamates. (c) The decarbamylation rate constant k_d is insensitive to the length of the carbamylenzyme. A similar insensitivity to acyl length is observed for rate-determining deacylation during LpL-catalyzed hydrolysis of lipid *p*-nitrophenyl esters of C_4–C_{12} in length (Burdette & Quinn, 1986). (d) *p*-Nitrophenyl substrates and lipid substrates, in particular triolein, react at the same LpL active site (Quinn et al., 1982).

It is important to note that the structure–reactivity trends described herein for interaction of LpL with carbamates are not compromised by interfacial effects (Smith & Pownall, 1984), since three assays of micelle formation failed to detect aggregation of any of the carbamate inhibitors. In addition, because the carbamates are potent inhibitors of LpL, inhibition assays were conducted at sufficiently low carbamate concentrations that solubilization in comicelles (e.g., with TX100) was not required. Therefore, the inhibition kinetics are for homogeneous LpL reactions, which makes their correlation with structure–reactivity effects of heterogeneous LpL reactions, such as hydrolysis of mixed micellar *p*-nitrophenyl esters (Burdette & Quinn, 1986) and phospholipids (Shinomiya et al., 1983), all the more remarkable. An unexpected observation is that the pseudo-first-order rate constant for inhibition of LpL by PNPOC and PNPDC shows a concave upward dependence on carbamate concentration. This unusual behavior may be due to homotropic cooperativity (Segel, 1975), since the active form of LpL is a dimer of identical subunits (Olivecrona et al., 1985). An alternate possibility is that each subunit possesses both an active site and an effector site, as suggested for phospholipase A_2 catalysis (Hendrickson & Dennis, 1984). Additional experiments on this activation effect observed at higher PNPOC and PNPDC concentrations are in progress.

A solvent isotope effect of 1.5 is observed for carbamylation of LpL by PNPOC. This isotope effect is similar in magnitude to that on k_{cat}/K_m, which measures rate-determining acylation, of LpL-catalyzed hydrolysis of *p*-nitrophenyl esters (Burdette & Quinn, 1986; Quinn, 1985). The origin of the isotope effect is probably that H243 of the active site functions as a general acid–base catalyst of carbamylation, as it does for acylation in Scheme I. Therefore, interaction of LpL with *p*-nitrophenyl *N*-alkylcarbamates recruits the catalytic machinery of the enzyme (Kovach et al., 1988), in that the active site histidine functions in inhibition in a manner that is mechanistically analogous to its role in the acylation stage of substrate turnover.

The second-order carbamylation rate constants in Table I for LpL interaction with PNPOC and PNPBC are about 10-fold and 80-fold smaller, respectively, than k^*_{cat}/K^*_m (which monitors acylation only) for hydrolysis of *p*-nitrophenyl caprylate (Burdette & Quinn, 1986). The decarbamylation rate constants, on the other hand, are $\sim 10^5$-fold smaller than the deacylation rate constant k^*_{cat} for turnover of *p*-nitrophenyl caprylate. Chart II compares carbamyl-LpL and acyl-LpL intermediates and provides a rationale for this 10^5-fold kinetic selectivity. The 10–80-fold lower carbamylation versus acylation reactivity likely comes from the fact that resonance delocalization of the carbamate nitrogen lone pair decreases the electrophilicity of the carbonyl function when compared to that of an ester. This effect should still operate in the

Chart II: Comparison of LpL Intermediates

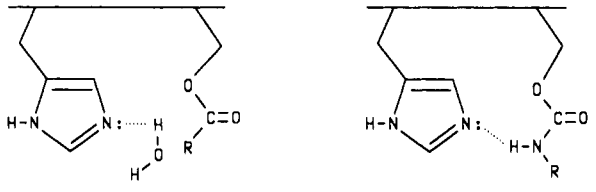

decarbamylation stage of the reaction, leaving a factor of 10^3–10^4 for which account yet must be made. As shown in Chart II, H-bonding between the carbamate NH and H243 of the active site should inhibit general base catalysis of decarbamylation by H243, whereas a similar H-bond is not possible in the acylenzyme intermediate. A typical H-bond strength 4–5 kcal mol^{-1} accounts for the residual kinetic specificity of 10^3–10^4.

LpL, like many lipolytic enzymes, showed enhanced activity when bound to lipid–water interfaces (Shirai & Jackson, 1983), though the molecular mechanism of this activation has not been elucidated. A possible explanation comes from comparison of the primary structures of bovine milk LpL (Senda et al., 1987) and human pancreatic lipase. Winkler et al. (1990) pointed out that the pancreatic lipase active site is covered in the crystal structure by a disulfide-bridged surface loop between residues C237 and C261. H263 is near the downstream end of this loop but points into the interior of the enzyme and joins S152 and D176 in the active site triad. Cysteines 218 and 241 are similarly positioned in bovine milk LpL adjacent to H243, which suggests equivalent functions for the discussed residues in LpL and pancreatic lipase. Hence, movement of the surface loop, which covers the catalytic triad with hydrophobic residues (Winkler et al., 1990), is required for ligand binding to and perhaps release from the LpL active site. One might expect that for carbamylenzymes and acylenzymes of increasing length, and hence hydrophobicity, interaction between the surface loop and the fatty acyl chain of the intermediate is increasingly favorable. Because the surface loop blocks access, diffusion of water into the active site, and perhaps release of products, should be increasingly impeded as fatty acyl length increases. If, as Winkler et al. (1990) suggest, movement of the surface loop is a structural determinant of interfacial activation, hydrolysis of longer carbamyl-LpLs (acyl-LpLs) should experience greater interfacial activations than shorter intermediates. We will report in due course experimental results on the mechanism of interfacial activation of LpL by micelles and vesicles that address this possibility.

Registry No. LpL, 9004-02-8; PNPBC, 63321-50-6; PNPDC, 132333-23-4; PNPOC, 63321-54-0; dodecylamine, 124-22-1; *p*-nitrophenyl chloroformate, 7693-46-1.

References

Andley, U. P., & Chakrabarti, B. (1981) *Biochemistry 20*, 1687–1693.

Blow, D. M. (1976) *Acc. Chem. Res. 9*, 145–152.

Borensztajn, J., Ed. (1987) *Lipoprotein Lipase*, Evener Publishers, Chicago.

Bradford, M. M. (1976) *Anal. Biochem. 72*, 248–254.

Brady, L., Brzozowski, A. M., Derewenda, Z. S., Dodson, E., Dodson, G., Tolley, S., Turkenburg, J. P., Christiansen, L., Huge-Jensen, B., Norskov, L., Thim, L., & Menge, U. (1990) *Nature 343*. 767–770.

Burdette, R. A., & Quinn, D. M. (1986) *J. Biol. Chem. 261*, 12016–12021.

Carey, M. C., & Small, D. M. (1969) *J. Colloid Interface Sci. 31*, 382–396.

Carpenter, B. K. (1984) *Determination of Organic Reaction Mechanisms*, pp 76–82, John Wiley & Sons, New York.

Chapus, C., & Sémériva, M. (1976) *Biochemistry 15*, 4988–4991.

Egelrud, T., & Olivecrona, T. (1973) *Biochim. Biophys. Acta 306*, 115–127.

Enerbäck, S., Semb, H., Bengtsson-Olivecrona, G., Carlsson, P., Hermansson, M.-L., Olivecrona, T., & Bjursell, G. (1987) *Gene 58*, 1–12.

Guidoni, A., Benkouka, F., De Caro, J., & Rovery, M. (1981) *Biochim. Biophys. Acta 660*, 148–150.

Hendrickson, H. S., & Dennis, E. A. (1984) *J. Biol. Chem. 259*, 5734–5739.

Hosie, L., Sutton, L. D., & Quinn, D. M. (1987) *J. Biol. Chem. 262*, 260–264.

Iverius, P.-H. (1971) *Biochem. J. 124*, 677–683.

Kirchgessner, T. G., Svenson, K. L., Lusis, A. J., & Schotz, M. C. (1987) *J. Biol. Chem. 262*, 8463–8466.

Kitz, R. J., Ginsburg, S., & Wilson, I. B. (1967) *Mol. Pharmacol. 3*, 225–232.

Komaromy, M. C., & Schotz, M. C. (1987) *Proc. Natl. Acad. Sci. U.S.A. 84*, 1526–1530.

Kovach, I. M., Huber, J. H., & Schowen, R. L. (1988) *J. Am. Chem. Soc. 110*, 590–593.

Kraut, J. (1977) *Annu. Rev. Biochem. 46*, 331–358.

Matsuoka, N., Shirai, K., & Jackson, R. L. (1980) *Biochim. Biophys. Acta 620*, 308–316.

Olivecrona, T., & Bengtsson, G. (1984) in *Lipases* (Borgström, B., & Brockman, H. L., Eds.) pp 205–261, Elsevier, Amsterdam.

Olivecrona, T., & Bengtsson-Olivecrona, G. (1987) in *Lipoprotein Lipase* (Borensztajn, J., Ed.) pp 15–58, Evener Publishers, Chicago.

Olivecrona, T., Bengtsson-Olivecrona, G., Osborne, J. C., & Kemper, E. S. (1985) *J. Biol. Chem. 260*, 6888–6891.

Polgár, L. (1987) in *Hydrolytic Enzymes* (Neuberger, A., & Brocklehurst, K., Eds.) pp 159–200, Elsevier, Amsterdam.

Quinn, D. M. (1985) *Biochemistry 24*, 3144–3149.

Quinn, D. M., Shirai, K., Jackson, R. L., & Harmony, J. A. K. (1982) *Biochemistry 21*, 6872–6879.

Quinn, D., Shirai, K., & Jackson, R. L. (1983) *Prog. Lipid Res. 22*, 35–78.

Salomaa, P., Schaleger, L. L., & Long, F. A. (1964) *J. Am. Chem. Soc. 86*, 1–7.

Savitsky, A., & Golay, M. J. E. (1964) *Anal. Chem. 36*, 1627–1639.

Schowen, K. B. J. (1978) in *Transition States of Biochemical Processes* (Gandour, R. D., & Schowen, R. L., Eds.) pp 225–283, Plenum Press, New York.

Segel, I. H. (1975) *Enzyme Kinetics*, pp 353–377, John Wiley & Sons, New York.

Senda, M., Oka, K., Brown, W. V., Qasba, P. K., & Furuichi, Y. (1987) *Proc. Natl. Acad. Sci. U.S.A. 84*, 4369–4373.

Shinomiya, M., McLean, L. R., & Jackson, R. L. (1983) *J. Biol. Chem. 258*, 14178–14180.

Shinomiya, M., Epps, D. E., & Jackson, R. L. (1984) *Biochim. Biophys. Acta 795*, 212–220.

Smith, L. C., & Pownall, H. J. (1984) in *Lipases* (Borgström, B., & Brockman, H. L., Eds.) pp 263–305, Elsevier, Amsterdam.

Stroud, R. M. (1974) *Sci. Am. 231* (1), 74–88.

Sutton, L. D., Stout, J. S., Hosie, L., Spencer, P. S., & Quinn, D. M. (1986) *Biochem. Biophys. Res. Commun. 134*, 386-392.
Twu, J.-S., Nilsson-Ehle, P., & Schotz, M. C. (1976) *Biochemistry 15*, 1904-1909.
Vainio, P., Virtanen, J. A., & Kinnunen, P. K. J. (1982) *Biochim. Biophys. Acta 711*, 386-390.
Verger, R. (1984) in *Lipases* (Borgström, B., & Brockman, H. L., Eds.) pp 83-150, Elsevier, Amsterdam.
Wentworth, W. E. (1965) *J. Chem. Educ. 42*, 96-103.
Winkler, F. K., D'Arcy, A., & Hunziker, W. (1990) *Nature 343*, 771-774.
Wion, K. L., Kirchgessner, T. G., Lusis, A. J., Schotz, M. C., & Lawn, R. M. (1987) *Science 235*, 1638-1641.
Zilversmit, D. B. (1977) *Adv. Exp. Med. Biol. 109*, 45-59.
Zilversmit, D. B. (1979) *Circulation 60*, 473-485.

Tissue-Specific and Hormonal Regulation of Human Prostate-Specific Glandular Kallikrein†

Charles Y.-F. Young,*,‡ Paul E. Andrews,‡ Benjamin T. Montgomery,‡ and Donald J. Tindall‡,§

Department of Urology and Department of Biochemistry and Molecular Biology, Mayo Clinic/Foundation, Rochester, Minnesota 55905

Received May 23, 1991; Revised Manuscript Received August 20, 1991

ABSTRACT: Kallikreins are involved in the posttranslational processing of a number of specific polypeptide precursors. Previously, human glandular kallikrein (hGK-1) mRNA has been identified in the prostate; however, the hGK-1 protein has not been identified and characterized. Therefore, its physiologic function in the prostate is not known. In this study, we have isolated a full-length hGK-1 cDNA from a human adenocarcinoma cell line, LNCaP. In vitro translation experiments demonstrated that the molecular size of the hGK-1 protein generated from this cDNA is similar to that of prostate-specific antigen (PSA), a protein which is produced exclusively in the prostate. In situ hybridization with a hGK-1-specific oligonucleotide probe (77 bases), which can differentiate hGK-1 mRNA from PSA mRNA, demonstrated the hGK-1 mRNA to be located in the prostate epithelium. The hGK-1 mRNA was colocalized with PSA mRNA in prostatic epithelia. Moreover, in situ hybridization studies revealed that the level of hGK-1 mRNA in human benign prostatic hyperplasia tissues is approximately half that of PSA mRNA. Furthermore, we have demonstrated that hGK-1 mRNA is under androgenic regulation in LNCaP cells. Time course analysis revealed that hGK-1 mRNA levels increased significantly at 5 h of mibolerone treatment and reached maximal levels by 9 h. In addition, hGK-1 mRNA levels were increased by dihydrotestosterone, but not by dexamethasone or diethylstilbestrol treatments. Flutamide, a nonmetabolized anti-androgen, repressed the androgenic effects. These studies suggest that expression of hGK-1 mRNA is regulated by androgen via the androgen receptor.

The glandular kallikreins are a subgroup of serine proteases which are involved in the posttranslational processing of specific polypeptide precursors to their biologically active forms (Clements, 1989). The rodent kallikrein gene family consists of at least 25 genes (Clements, 1989; Mason et al., 1983; Wines et al., 1989). However, the human kallikrein gene family is much smaller, consisting of three well-described members (Clements, 1989; Schedlich et al., 1987): prostate-specific antigen (PSA),[1] glandular kallikrein (hGK-1), and pancreatic/renal kallikrein (hPRK).

Deduced amino acid sequences indicate that hGK-1 may be a trypsin-like serine protease (Schedlich et al., 1987; Morris, 1989) whereas PSA is a chymotrypsin-like serine protease (Lilja, 1983; Watt et al., 1986). Therefore, these two genes may have different physiological functions. The cDNA and genomic sequences for PSA and hPRK have been reported (Lundwal & Lilja, 1987; Lundwall, 1989; Fukushima et al., 1985; Evans et al., 1988), but only the genomic sequence for hGK-1 is available (Schedlich et al., 1987). The DNA sequence homology between hGK-1 and PSA (exon regions) is 80%, whereas the homology between hGK-1 and hPRK is 65% (Schedlich et al., 1987; Morris, 1989). The amino acid sequence homology of hGK-1 with PSA and hPRK is 78% and 57%, respectively (Schedlich et al., 1987; Morris, 1989). The similarities of gene structure and deduced amino acid sequences of these human kallikreins suggest that their evolution may involve the same ancestral gene. Moreover, both hGK-1 and PSA are expressed only in the human prostate (Morris, 1989; Chapdelaine et al., 1988). Expression of hPRK is limited to the pancreas, submandibular gland, kidney, and other nonprostate tissues (Morris, 1989). Interestingly, the hGK-1 gene is located about 12 kbp downstream from the PSA gene in a head-to-tail fashion on chromosome 19 (Riegman et al., 1989). Thus, the relationship between hGK-1 and PSA gene expression is very intriguing, especially with respect to their

† This work was supported partly by Grants DK41995 (to C.Y.-F.Y.) and CA32387 (to D.J.T.) from the National Institutes of Health.
* To whom correspondence should be addressed.
‡ Department of Urology.
§ Department of Biochemistry and Molecular Biology.

[1] Abbreviations: hGK-1, human glandular kallikrein; PSA, prostate-specific antigen; hPRK, pancreatic/renal kallikrein(s); SDS, sodium dodecyl sulfate; BPH, benign prostatic hyperplasia; EDTA, ethylenediaminetetraacetic acid; PAGE, polyacrylamide gel electrophoresis.

0006-2960/92/0431-818$03.00/0